Roughness characterization of the galling of metals

Cédric Hubert, Julie Marteau, Raphaël Deltombe, Y Chen, Maxence Bigerelle

Roughness characterization of the galling of metals

Roughness characterization of the galling of metals

C Hubert[1,2], J Marteau[1,3], R Deltombe[1,3], Y M Chen[4] and M Bigerelle[1,2]

[1] Univ Lille Nord de France, F-59000 Lille, France
[2] UVHC, TEMPO EA 4542, F-59313 Valenciennes, France
[3] UVHC, LAMIH UMR CNRS 8201, F-59313 Valenciennes, France
[4] CETIM, F-60304 Senlis, France

E-mail: cedric.hubert@univ-valenciennes.fr

Abstract

Several kinds of tests exist to characterize the galling of metals, such as that specified in ASTM Standard G98. While the testing procedure is accurate and robust, the analysis of the specimen's surfaces (area = 1.2 cm) for the determination of the critical pressure of galling remains subject to operator judgment. Based on the surface's topography analyses, we propose a methodology to express the probability of galling according to the macroscopic pressure load. After performing galling tests on 304L stainless steel, a two-step segmentation of the S_q parameter (root mean square of surface amplitude) computed from local roughness maps (100 μm × 100 μm) enables us to distinguish two tribological processes. The first step represents the abrasive wear (erosion) and the second one the adhesive wear (galling). The total areas of both regions are highly relevant to quantify galling and erosion processes. Then, a one-parameter phenomenological model is proposed to objectively determine the evolution of non-galled relative area A_e versus the pressure load P, with high accuracy ($A_e = 100/(1 + aP^2)$ with $a = 0.54_{\pm 0.07} \times 10^{-3}\,\mathrm{MPa}^{-2}$ and with $R^2 = 0.98$). From this model, the critical pressure of galling is found to be equal to 43MPa. The $S_{5\,V}$ roughness parameter (the five deepest valleys in the galled region's surface) is the most relevant roughness parameter for the quantification of damages in the 'galling region'. The significant valleys' depths increase from 10 μm–250 μm when the pressure increases from 11–350 MPa, according to a power law ($S_{5\,V} = 4.2P^{0.75}$, with $R^2 = 0.93$).

Keywords: galling, seizure, roughness, stainless steel, fractal analysis

1. Introduction

A lot of mechanical equipment requires assembly components to slide against each other, e.g., pump wear rings, valve stems, and engine pistons. These systems are often prone to catastrophic adhesion-initiated wear, whether they are lubricated or not. Several words are used in tribology to denote catastrophic wear under different conditions. The most common are: seizure [1–3], galling [4, 5], and scuffing [6, 7]. Markov and Kelly [8, 9] defined some of the terms used to describe adhesion-initiated catastrophic wear. According to their review of past technical usage of these terms, seizure seems to be a general term used for the damage of friction surfaces. Scuffing is often used to define the wear of lubricated surfaces, while galling refers to the wear of non-lubricated surfaces. This paper will focus on galling only.

According to ASTM Standard G40 [10], galling is 'a form of surface damage arising between sliding solids, distinguished by macroscopic, usually localized, roughening and creation of protrusions above the original surface; it often includes plastic flow or material transfer, or both'. Currently, ASTM Standard G98 [11] is the only standard for defining the galling resistance of materials. This test method, called the button-on-block test, requires maintaining a constant compressive load between the specimens while one specimen is slowly rotated against the other. The specimens are then visually inspected for the presence of galling. Some characteristic features of galling are described in the standard to

help the determination of the onset of galling. However, it remains a subjective assessment.

Most of the literature on galling focuses on the understanding of adhesion-initiated wear [12, 13] or on the identification of the phenomena or factors leading to galling [14–16]. Few studies examine the quantification of galling; i.e., few tried to use roughness measurements in order to estimate the contact area that undergoes galling. As an example, Hummel and Partlow [17] compared threshold galling results using two testing methods, the button-on-block test and a line contact testing procedure. For the button-on-block test, they defined the threshold galling stress as the magnitude of stress required such that 50% of the specimens tested at that level would show roughening and raised protrusions (without the assistance of magnification). Despite this new definition, Hummel and Partlow concluded that a more robust method was required to calculate galling threshold stress. Andreason *et al* [18] quantified galling by surface roughness analysis in order to compare different lubricants. They proposed identifying the onset of galling by observing the first significant deep valley resulting from the test. Their method enabled a certain quantification of galling but was dedicated to lubrication tests. In this paper, a new methodology is presented for the quantification of galling, based on ASTM Standard G98. This new method enables one to differentiate the galled region from the eroded region without operator bias. Thanks to this identification, the percentile of galled and eroded area can be calculated. The latter is then used to determine a relation between the load and the percentile of the eroded area.

This article is divided into three sections. The first one is dedicated to the introduction of the experimental galling tests and to visual examinations of the tested specimens; the second one describes the methodology to differentiate the eroded and galled regions; and the third section is attached to the determination of the relationship between the eroded region and the applied load to give a more deterministic feature to galling tests.

2. Design of experiments

The experiments carried out in this study are based on ASTM Standard G98 [11]. As described in the introduction, this galling test is a button-on-block test, which consists of the application of a constant normal force on the button in contact with the block surface while it is rotated. The button rotation is limited to one revolution, which, according to the ASTM standard, must be performed in 3 s–20 s in a single step. The testing device is a standard tensile-compression machine with a maximum load of 250 kN coupled to a controlled gear motor to apply the button revolution. The normal force and the torque are recorded by means of a numerical recorder. A picture of the testing device and a schema of the specimens (shown reversed for understanding) are given in figures 1(a) and (b), respectively.

In this study, six buttons were used to perform tests with six different normal forces, on six different locations on the block, as illustrated in figure 1(b). The buttons and block material are AISI 304L stainless steel. The contacting surfaces were prepared by turning then finishing by grinding, leading to a surface roughness of $S_a = 0.4\ \mu$m, as specified by the standard. For a given specimen, the different testing steps are as follows:

1. application of the chosen load;
2. application of one revolution of the button during the chosen time;
3. release of the normal load.

The apparent pressures, calculated as the load to button area ratio corresponding to each normal load applied in this study, are given in table 1.

At the end at each test, the specimen is visually examined. According to ASTM Standard G98, galling has occurred if the contacting surfaces exhibit torn metal. The results of the experiments are shown in figure 2.

Figure 2(a) shows all buttons associated to the trace left on the block during the tests. For Test N°1, with applied pressure of 11 MPa, the initial surface is almost unchanged and exhibits only very small scratches. According to ASTM Standard G98, this does not correspond to galling. In the case of these experiments, visually, the onset of galling seems to occur for Test N°2, with a normal pressure of 22 MPa (figure 2(b)). Tests ranging from N°3–N°6 exhibit an increasing area with torn material, logically indicating more galling with increased pressure.

This kind of observation, as specified by the standard, is visual with 'unaided eye' and is thus subjective. As described in the introduction, the remainder of this paper is focused on finding a more deterministic way to quantify the onset of galling. This will be achieved by means of surface topography analyses, presented in the next section.

3. Surfaces topography analyses

To quantify the occurrence of galling, corresponding to severe deformation of the contacting surfaces, the surfaces' topography must be analysed. This analysis will be achieved in two main steps. The first one will allow us to determine if a given tested region has undergone severe deformations or not; i.e., if this surface has kept its initial topographical features, and at which conservation level. In the second step, this conservation level will be expressed in terms of area of the eroded region, giving an estimation of the galling severity, which will be related to the corresponding testing pressure in section 4 of this paper.

3.1. Initial surface analysis

The starting point of the surfaces' topography analyses is to define the relevant analysis scale, which is required to assess that the observed topographical parameters are calculated at a scale that is consistent with the studied process. It must be achieved on surfaces before testing, and since all surfaces are

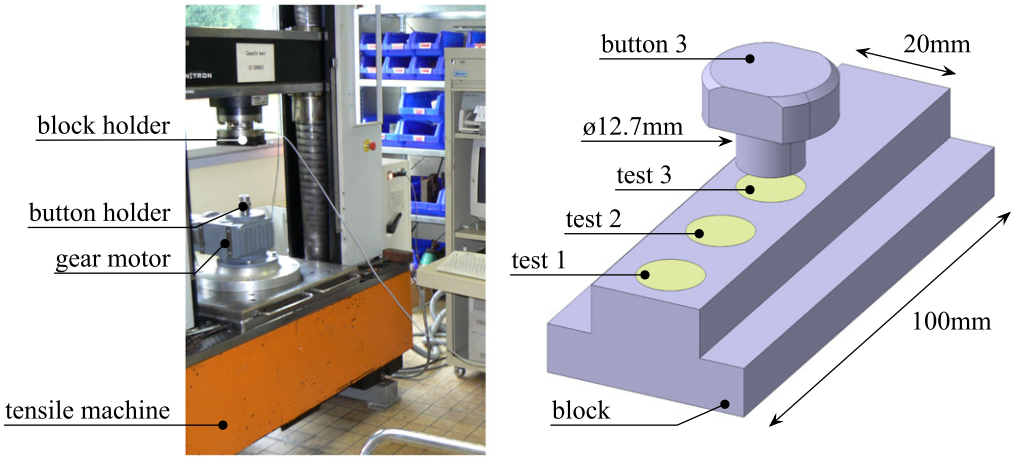

Figure 1. Testing device (a) and specimens illustration with main dimensions, in reversed position (b).

Table 1. Testing conditions with corresponding apparent pressures.

Test N°	1	2	3	4	5	6
Pressure (MPa)	11	22	44	88	172	350

made with the same material, prepared with the same process in one step, only one surface will be analysed.

All surfaces involved in this study were measured with a Zygo NewView 7300 3D optical surface profiler. This device has a vertical resolution of 0.1 nm that only depends on the piezoelectric stage and an in-plane resolution of 2.2 μm related to the ×5 magnification objective used for the purpose of this study. All surfaces were measured by stitching, consisting of performing several measurements to cover the whole desired surface, with a surface overlap between each acquisition of 30%. After reconstruction of all independent images, the full image can be analysed.

The roughness parameter chosen to quantify the conservation level between the initial and tested surfaces is the S_q, which is very similar to the S_a, but more sensitive to peaks and valleys, since the amplitudes are squared. The relevant analysis scale was determined by fractal analysis on the initial surface S_q map. Figure 3(a) shows a randomly chosen region of the block surface before the galling test, after shape removal and thresholding, and figure 3(b) shows the map of the S_q parameter.

In figure 3(b), the S_q parameter was calculated on the entire map of the surface in figure 3(a), with a floating window of a given size, to create a map of this parameter. To obtain the presented map, the window size used was a square area with dimensions of 7×7 pt^2 (15.4×15.4 μm^2). It corresponds to a voluntarily very small window size, and the measured value of the S_q may be related to the roughness of scratches resulting from the abrasive finishing process. Thus, the S_q parameter must be evaluated at a scale which is small enough to catch morphology changes due to galling, but also large enough to be independent from the finishing process.

To determine what is the best observation scale for the S_q roughness parameter, a fractal analysis was performed on the S_q map shown in figure 3(b). The method used is based on morphological opening and closing of a flat structuring element to calculate the lower and upper envelopes of the analysed surface, i.e., the S_q map. The procedure is repeated for different sizes of the structuring element and allows us, at the end of the process, to build a graph that expresses the enclosed volume versus the structuring element size in logarithmic scale. The graph obtained for the fractal analysis of the S_q map shown in figure 3(b) is given in figure 4.

In the log–log plot of figure 4, the slope α corresponds to the fractal dimension, where $D = 3 - \alpha$ is the fractal dimension of the shape using the Bouligand–Minkowski method [19]. Two linear trends (a 'biplot') can be visually observed that correspond to a fractal dimension change. When fitting the two extreme parts of this scale law by two power laws, represented by straight lines on the graph of figure 4, an intersection is obtained, assumed as a critical point of regime change of the S_q parameter, as observed in [20, 21]: at low scale, below this critical point, the observed values of S_q correspond to the roughness of the surface finishing process, while at higher scales, the S_q values are more related to the overall surface. This threshold is linked to the influence of the abrasion region due to contact between grains and surfaces [22].

This regime change occurs for an observation scale of about 0.1×0.1 mm^2. In this study, the window size used to calculate the S_q maps for the tested surfaces takes into account the effect of the observation scale and was set to 47×47 pt^2 (the edge size must be odd since the window is centred on a surface point), corresponding to 103×103 μm^2.

The S_q map recomputed using the determined relevant observation scale is given in figure 5(a), and the distribution of the S_q map amplitudes is plotted in figure 5(b).

The graph of figure 5(b) shows that most of the S_q map amplitudes range in [0.1; 0.4] μm, and the highest value is

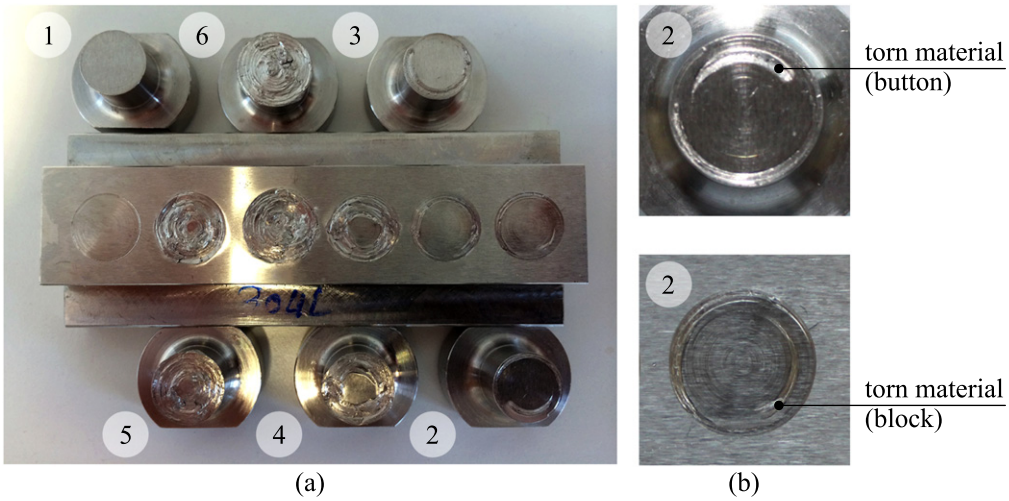

Figure 2. Buttons and block after galling tests (a), and magnification of the contacting surfaces for Test N2 (b).

close to 0.7 μm. Since it is assumed that this surface is representative of the whole set of initial surfaces, any S_q value which, after testing, is greater than the maximal value observed on the initial surface would correspond to deformed regions of the surface. It is obvious that any contact on the initial surface modifies its roughness, even if no galling occurs. Eroded regions would thus correspond to 'slightly deformed' surfaces, with S_q values slightly greater than the initial one. Galled regions result in strong changes in the surfaces roughness that should be clearly highlighted by the S_q amplitudes' distribution, thanks to the fractal analysis, which ensures the right observation scale.

This critical value of the initial S_q map is used in the next section of the study to determine the regions affected by a morphology change due to the galling test and to estimate the area of the eroded and galled regions.

3.2. Final surfaces analysis

The surfaces obtained after the galling test were measured following the same method and the same parameters as those used for the acquisition of the initial surface in section 3.1. Both the buttons and the block traces were measured, except for Test N°3, in which difficulties have been encountered with the button. Thus, 11 measurements instead of 12 will be used for the remainder of the study. The aim of this section is to differentiate the eroded regions from the galled regions, with the objective their respective areas. From the analysis performed on the initial surface (section 3.1), it is now established that regions of the buttons/block traces which have S_q values close to the initial ones will belong to the eroded regions, and the values greater than the initial ones will be attributed to galled regions. This argument is first applied to the contacting surfaces resulting from Test N°4, which exhibits strong surface changes in the peripheral region of both the button and the block trace (figure 2(a)), while the centre regions seem, visually, to remain unchanged. Figure 6 shows the S_q map of the block trace (figure 6(a)) and the button surface (figure 6(b)), both calculated with a window size of 47×47 pt^2, and their respective heights distribution histogram.

The S_q maps in figure 6, in conjunction with the plots of the distributions of the S_q values, confirm the visual observations above: the values of the S_q parameter in the centre of the contacting surfaces are close to zero, corresponding to the highest bins in the histograms (lower than 1 μm, as determined in section 3.1), while the peripheral regions exhibit an increase of the initial roughness, with S_q values mainly ranging in [1; 10] μm (amplitudes greater than 40 μm have been hidden). The histograms of both surfaces also show a break in the S_q values distribution located at 1 μm, denoting the transition between values of S_q belonging to the eroded and galled regions.

Based on the S_q value of this break, the eroded and galled regions may now be objectively split up by thresholding the S_q maps, then applying a mask to the surfaces' topography. This operation results in two sub-surfaces for the block and the button, as illustrated in figure 7, containing the eroded and galled regions. The areas corresponding to each region may now be calculated, giving an eroded region of 24.4 mm^2 and a galled region of 102.1 mm^2 for the block trace, corresponding to 19.5% and 80.5% of the measured surface area. For the button, the area of the eroded region is 29.7 mm^2, and the area of the galled region is 95.4 mm^2, corresponding to 24% and 76% of the measured surface area, respectively.

Applying the same methodology to the overall set of surfaces gives table 2. Anticipating the remainder of the study, and since both measurements are complementary, the results will be expressed in terms of eroded region area.

4. Relationship between galling and testing pressure

4.1. Relevance of the eroded region area

The results obtained in the previous section give important information on the amount of galled material resulting from the test and can be expressed as a function of the applied

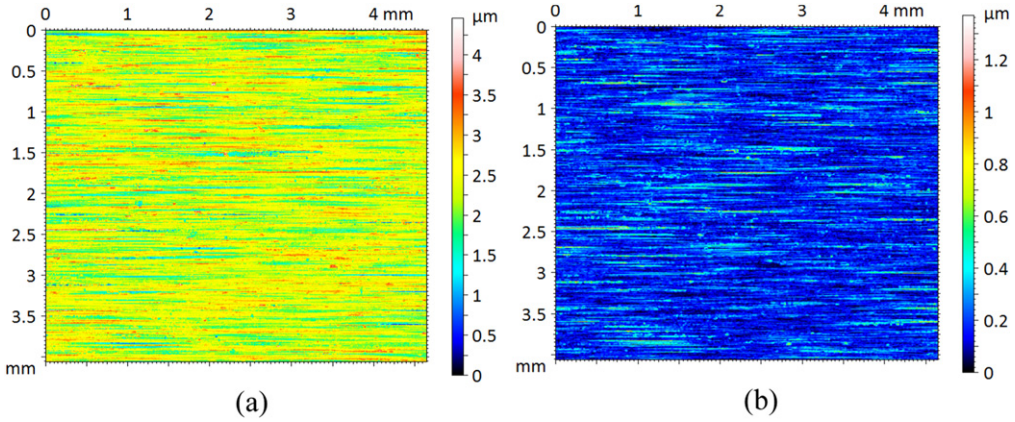

Figure 3. Initial surface acquired on the block (a) and map of the S_q roughness parameter (b).

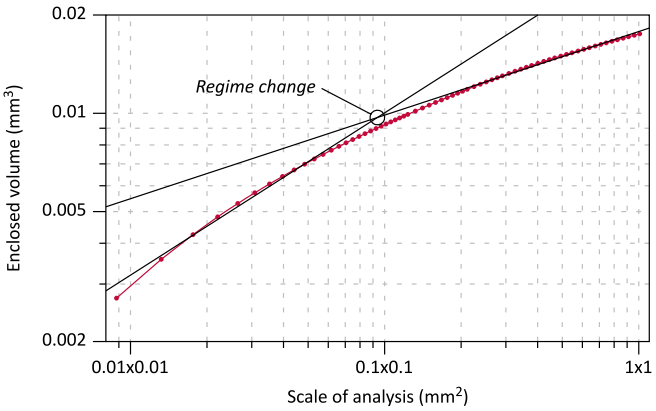

Figure 4. Result of the fractal analysis of the S_q map shown in figure 3(b).

pressure. The area of the eroded region is intuitively an important parameter, but its relevance to quantify the occurrence and amount of galling is not yet established; i.e., if the eroded area is sufficient on its own to discriminate two galled specimens.

In order to validate this assumption, this parameter was to be submitted, along with other roughness parameters, to a relevance analysis. It was performed by a computer software program called MESRUG® [23] that allows us to calculate a large number of roughness parameters, standard or not, and to statistically estimate their relevance according to any particular functional property. The relevance of each parameter is estimated by means of a one-way analysis of variance procedure then plotted on a graph.

Figure 8 shows the relevance graph resulting from the relevance analysis performed on 250 parameters, in which the abscissa corresponds to the tested parameters, sorted in relevance descending order, and the ordinate corresponds to the value of the parameters' relevance.

As expected, according to the graph of figure 8, the area of the eroded region A_e is a good parameter to quantify the occurrence of galling, since it decreases as the testing pressure increases and thus avoids any confusion between two specimens tested with different pressures. Two other parameters are also relevant: the topographical parameter S_{5v} and the functional parameter V_v. The S_{5v} parameter, which is analogous to the S_v, corresponds to the average value of the five deepest valleys in the galled region's surface. According to the relevance analysis results, it is the second most relevant parameter; it characterizes the torn material amplitude. The third most relevant parameter is the void volume V_v, calculated on the galled region's surface. It characterizes the volume of metal protrusions, which may be more accurate than the S_{5v} with less ductile metals, which may produce shallower protrusions.

Each of these three parameters are plotted on separate graphs in figure 9 as a function of the testing pressure, with their global trend given by MESRUG®.

From the graphs of figure 9 it can be seen that the parameters exhibit an asymmetry between the buttons and their plate counterpart. It is supposed that the tests, in addition to galling, also lead to the formation of a third body, which may have been removed during the cleaning and manipulation processes. Moreover, the ASTM Standard G98 imposes a full revolution of the specimens during the test, which may lead to re-flattening of the created asperities and thus changes of the surface's topography between the plate and the button.

On one hand, concerning parameter S_{5v}, the graph of figure 9(b) shows a mostly linear trend, meaning that the amount of galled material between two contacting surfaces evolves linearly with the pressure. This seems contradictory to the study conducted by Hummel and Partlow [17] that showed a fast increase of the galled area with pressure then a stabilisation at a high level of the galled area for the remaining testing pressures, leading to the onset of galling being a particularly sensitive phenomenon. On the other hand, the V_v parameter has an exponential global trend, which may be more suitable for representing the sensitive feature of galling occurrence. Comparing this roughness parameter to the eroded area (A_e, discussed below) or the S_{5v}, two groups of tests can be highlighted: Tests N°1–3 have very small V_v values (less than 50 $\mu m^3\,\mu\,m^{-2}$), while the computed void volume is much higher for Tests N°4–6, which ranges in [150; 200] $\mu m^3\,\mu\,m^{-2}$. This behaviour may be considered as a transition between erosion and galling phenomena. Nevertheless, points corresponding to Tests N°4–6 show a

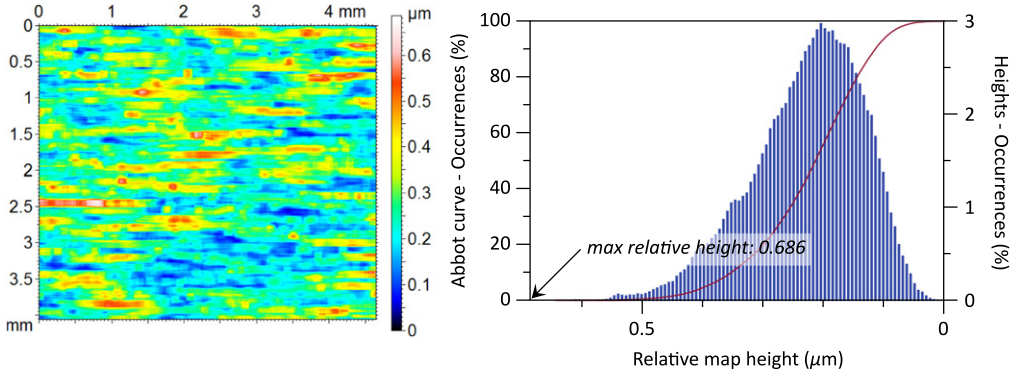

Figure 5. S_q map based on the relevant observation scale (a) and relative map heights distribution (b).

decreasing trend, which may be inconsistent with the prediction of galling phenomenon, since increasing the testing pressure would lead to less torn material.

On the contrary, the evolution of the eroded region area A_e shows a monotonic descending trend with a steep slope between Test N°2 and N°4 that relates the sensitive property illustrated by the Hummel and Partlow measurements [17]. As visually observed, the surfaces resulting from Test N°1 would not undergo galling, while Tests N°5–6 exhibit severe material protrusions, whatever the increase of testing pressure.

In the case of this study, the area of the eroded region seems to be definitely the most relevant parameter to differentiate the eroded and galled regions.

4.2. One-parameter phenomenological model to predict the amount of galling

As described in the introduction of this paper, ASTM Standard G98 recommends analysing the surfaces resulting from galling tests by simple visual observations with the unaided eye. From the analysis performed in the previous sections, it seems obvious that these visual observations may be improved, mainly thanks to the estimation of the eroded or galled regions' areas.

Based on the trend curve plotted on the graph in figure 9(a), a simple analytical phenomenological model can be built to estimate the onset of galling. This model must obviously satisfy $A_e \in [0; 100]\%$, where 0% corresponds to completely galled surfaces, and 100% corresponds to surfaces with small scratches not comparable to galling. This model reads:

$$A_e = 100 \times \frac{1}{1 + aP^2}, \tag{1}$$

where A_e is the percentile of eroded area, P is the testing pressure, and a is a parameter to be determined. For the material and testing pressure sets used in this study, a regression analysis on the model parameter a leads to $a = 0.\,54_{\pm 0.07} \times 10^{-3}\,\mathrm{MPa}^{-2}$.

As shown on the graph of figure 10, the model exhibits a maximal value corresponding to no occurrence of galling with zero pressure and decreases rapidly, validating the sensitive feature of galling, until reaching a pressure of 60–80 MPa. Then, the area of the eroded region decreases softly, eventually with an asymptotic value at 0%.

Using equation (1), and assuming a critical galling state corresponding to a galled region area of 50% as observed in Hummel and Partlow's study [17], the critical galling pressure reads:

$$P_{c50\%} = 1/\sqrt{a}\,. \tag{2}$$

For two contacting 304L stainless steel specimens, this critical pressure is $P_{c50\%} = 43$ MPa and corresponds, for the present set of experiments, to Test N°3, performed with $P = 44$ MPa.

5. Conclusions

The presented study aims to give a more deterministic feature to galling tests such as that governed by ASTM Standard G98, in which the occurrence or not of galling is determined by visual inspection of the tested specimens.

After determination of the relevant analysis scale by fractal analysis on the S_q map of the initial specimens' surface, an S_q roughness threshold was determined, allowing us to differentiate the eroded regions from the galled region. The application of this threshold to the tested surfaces enabled the calculation of the area of eroded material, which was then linked to the testing pressure. Finally, after assessment that this area of eroded material is the most relevant parameter to differentiate the eroded and galled regions of the specimens' surfaces, a one-parameter phenomenological model was built to express the area of eroded material with respect to the testing pressure.

This phenomenological model, even if it is identified on one set of experimental tests, allows us to give a more theoretical meaning to the effect of pressure on galling phenomena and allows us to reduce the operator bias when estimating the onset of galling.

The relevance of the previous methodology and results will have to be confirmed through the enrichment of the experimental data: several types of materials need to be tested

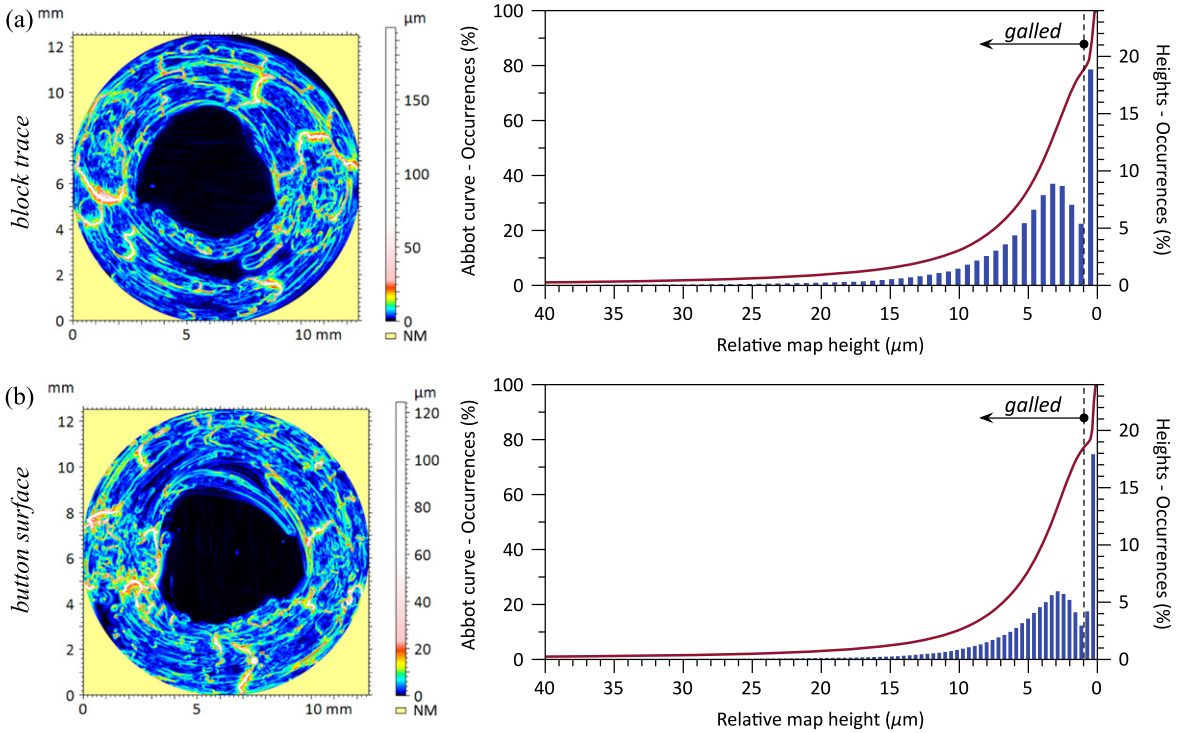

Figure 6. S_q maps and amplitudes distributions of the contacting surfaces of Test N°4: block trace (a) and button surface (b).

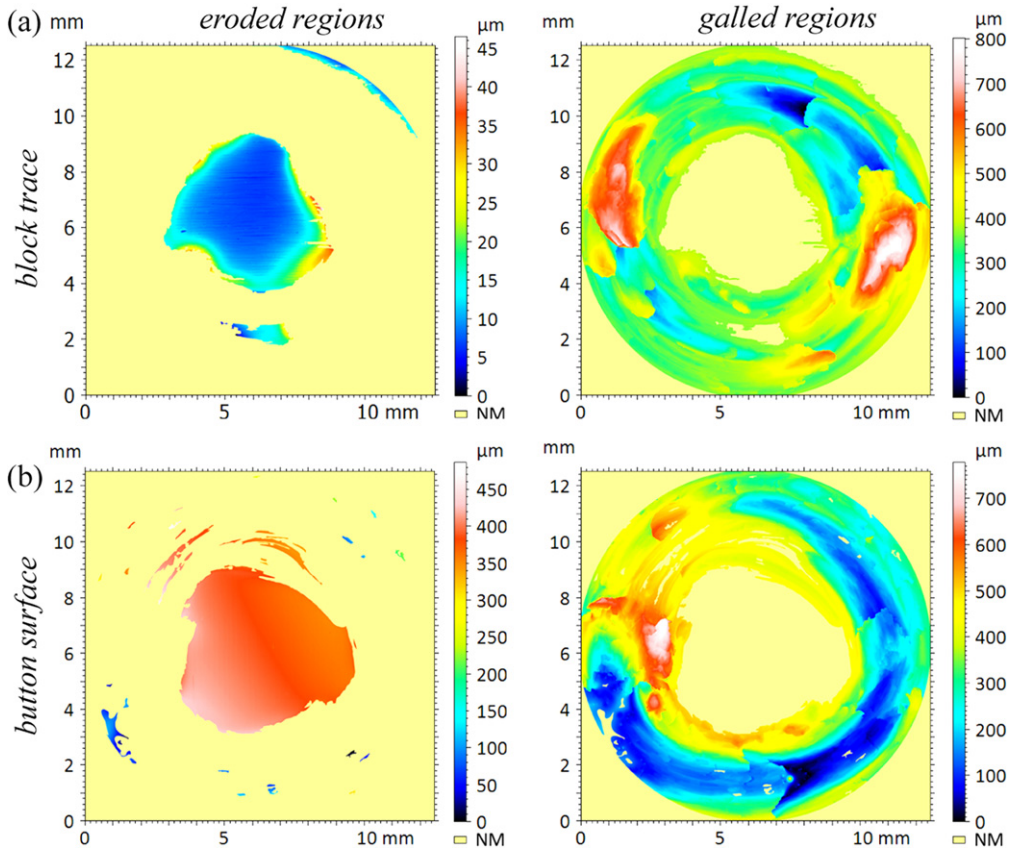

Figure 7. Eroded and galled regions topography for the block trace (a) and the button surface (b), Test N°4.

Table 2. Results of the calculation of the eroded area per test number, in percentile of the overall area.

Test N°	1	2	3	4	5	6
Block trace eroded area (%)	87.6	75.8	58.2	19.5	3.7	1.1
Button eroded area (%)	97.7	65.3	N/A	24	5.1	3.2

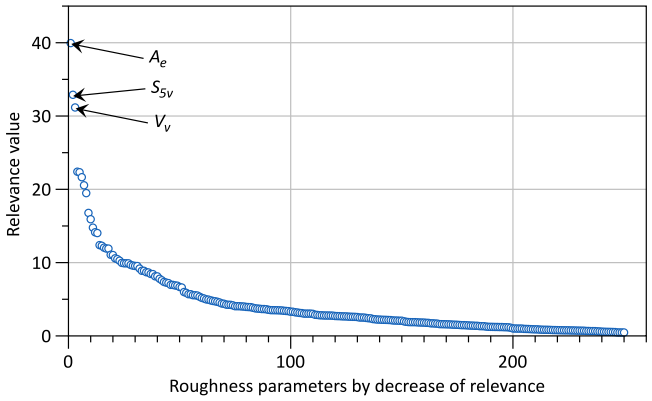

Figure 8. Results of the relevance analysis performed with MESRUG®.

in order to cover a broad range of materials used in engineering systems. The indentation model developed by Marteau *et al* [24, 25] may be helpful for the validation of the presented methodology. Indeed, this model enables us to make indentation tests despite large topography variations. A link may be found between the scatter of the indentation curves and the areas showing galling or erosion, which may lead to the determination of galling features.

Further investigations should also take into account the revolution velocity and the velocity gradient between regions close to the button centre and its perimeter. Moreover, increasing the tests' revolution velocity will probably lead to consideration of the temperature effects—namely, the materials' initial temperature and self-heating effects, which generally occur in many engineering applications.

Acknowledgments

The present research work has been supported by the ANR Sinus Surf 'SVSE 5 — Physique, chimie du vivant et innovations biotechnologiques (Blanc SVSE 5) 2012'.

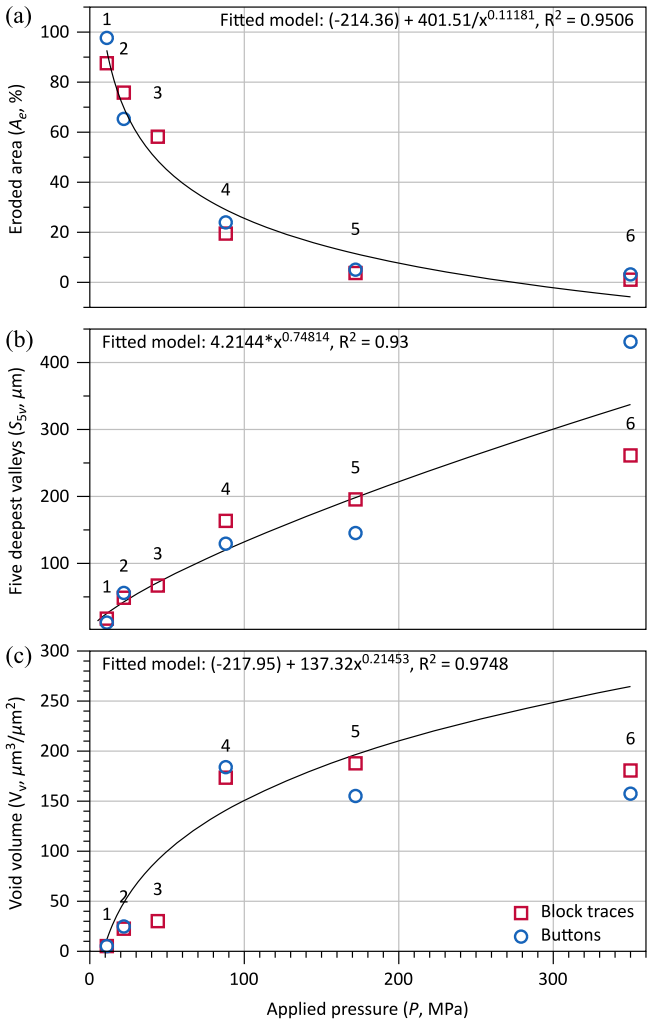

Figure 9. Evolution of parameters A_e (a), S_{5v} (b), and V_v (c), according to the testing pressure.

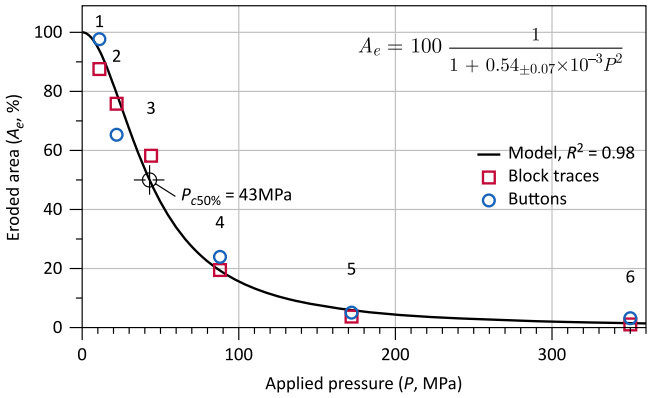

Figure 10. Plot of the built phenomenological model, expressing the eroded region area according to the testing pressure.

References

[1] Trent E M 1988 Metal cutting and the tribology of seizure: I seizure in metal cutting *Wear* **128** 29–45
[2] Trent E M 1988 Metal cutting and the tribology of seizure: II movement of work material over the tool in metal cutting *Wear* **128** 47–64
[3] Trent E M 1988 Metal cutting and the tribology of seizure: III temperatures in metal cutting *Wear* **128** 65–81
[4] Bernick L M, Hilsen R R and Wandrei C L 1978 Development of a quantitative sheet galling test *Wear* **48** 323–46
[5] Schedin E 1994 Galling mechanisms in sheet forming operations *Wear* **179** 123–8
[6] Jeong S H, Shin Y H, Kim H J, Song S J and Lee Y Z 2007 A study on scuffing and transition of friction and wear of tin films using ultrasonic backward radiation *Wear* **263** 1386–9

[7] Wang Y and Tung S C 1999 Scuffing and wear behavior of aluminum piston skirt coatings against aluminum cylinder bore *Wear* **225-229** 1100–8
[8] Markov D and Kelly D 2000 Mechanisms of adhesion-initiated catastrophic wear: pure sliding *Wear* **239** 189–210
[9] Markov D 1997 Laboratory tests for seizure of rail and wheel steels *Wear* **208** 91–104
[10] ASTM tandard G40 (2013). Standard Terminology Relating to Wear and Erosion ASTM International, West Conshohocken, PA, 1999, DOI: 10.1520/G0040 (http://www.astm.org)
[11] ASTM Standard G98 (2009). Standard Test Method for Galling Resistance of Materials International, West Conshohocken, PA, 2002, DOI: 10.1520/G0098-02R09 (http://www.astm.org)
[12] Rabinowicz E 1973 Friction seizure and galling seizure *Wear* **25** 357–63
[13] Yin X and Komvopoulos K 2010 An adhesive wear model of fractal surfaces in normal contact *Int. J. Solids Struct.* **47** 912–21
[14] Safara Nosar N and Olsson M 2013 Influence of tool steel surface topography on adhesion and material transfer in stainless steel/tool steel sliding contact *Wear* **303** 30–39
[15] Hirasaka M and Nishimura H 1994 Effects of the surface micro-geometry of steel sheets on galling behavior *J. Mater. Process. Technol.* **47** 153–66
[16] Podgornik B and Jerina J 2012 Surface topography effect on galling resistance of coated and uncoated tool steel *Surf. Coat. Technol.* **206** 2792–800
[17] Hummel S R and Partlow B 2004 Comparison of threshold galling results from two testing methods *Tribol. Int.* **37** 291–5
[18] Andreasen J L, Bay N and de Chiffre L 1998 Quantification of galling in sheet metal forming by surface topography characterisation *International Journal of Machine Tools and Manufacture* **38** 503–10
[19] Falconer K J 2014 *Fractal Geometry: Mathematical Foundations and Applications* 2nd edn (Chichester, UK: Wiley) chapter 15 (Random Fractals) doi:10.1002/0470013850.ch15
[20] Wu J-J 2000 Characterization of fractal surfaces *Wear* **239** 36–47
[21] Bigerelle M, Gautier A, Hagege B, Favergeon J and Bounichane B 2009 Roughness characteristic length scales of belt finished surface *J. Mater. Process. Technol.* **209** 6103–16
[22] Pohrt R and Popov V L 2013 Contact stiffness of randomly rough surfaces *Scientific Reports* **3** 3293
[23] Hennebelle F, Najjar D, Bigerelle M and Iost A 2006 Influence of the morphological texture on the low wear damage of paint coated sheets *Progress in Organic Coatings* **56** 81–89
[24] Marteau J, Bigerelle M, Xia Y, Mazeran P-E and Bouvier S 2013 Quantification of first contact detection errors on hardness and indentation size effect measurements *Tribol. Int.* **59** 154–62
[25] Xia Y, Bigerelle M, Marteau J, Mazeran P-E, Bouvier S and Iost A 2014 Effect of surface roughness in the determination of the mechanical properties of material using nanoindentation test *Scanning* **36** 134–49